Discussion

We have applied a simple mathematical model to quantitatively characterize the *in vitro* kinetics of SHIV-KS661 virus infection in HSC-F cell cultures, leveraging experimental data for total and infectious viral load, along with target and infected cell dynamics, to fully parameterize the system. Specifically, we determined values for the rate of loss of infectivity and the RNA degradation rate of SHIV-KS661, the target and infected HSC-F cell half-life, the rate constant for infection of target cells and the infectious and total viral production rates of infected cells. From these fundamental quantities, we also estimated a number of important derived quantities, including the burst size of an infected cell and the basic reproductive number. Additionally, by measuring both the total and infectious viral load within the context of a mathematical model we were able to provide a lower bound for the proportion of infectious virions produced by infected cells.

We estimated the half-life of SHIV-infected HSC-F cells to be *14.1* h. In clinical studies of patients or animals, it is extremely difficult to continuously measure the number of infected cells during infection. This is because the amount of infected cells in peripheral blood (PB) is very small. For example, in HIV-1 infected patients, there are only about 10^2 infected cells per 10^6 peripheral blood mononuclear cells at their set point [14]. Thus, measuring the number of infected cells in PB during the early phase of infection is technically difficult. In HIV-1 humanized mice, infected cells in PB are not detectable even during the acute phase when 80-90% of target cells in the spleen and lymph nodes are infected (K. Sato and S. Iwami, unpublished data). For this reason, the death rate of infected cells *in vivo* has primarily been estimated from the viral load decay (or the decay of infectious virus) after the peak of an acute infection [11,16,17,20,27] or after antiviral drug administration [10,14,15,22]. The maximum half-lives of HIV-1 and SIV-infected cells were both initially estimated - by analysis of *in vivo* viral decay under antiviral therapy - to be ~24 h [14,27], but drug combinations with higher efficacy have reduced the estimates to ~17 and ~11 h, respectively [12,22,44]. Our *in vitro* estimate of the half-life, based on direct observations of Nef-positive cell decay, agrees well with these indirect *in vivo* measures, despite the absence of immune effects.

We determined an SHIV-KS661 viral burst size of 2.21×10^4 RNA or *0.19* $TCID_{50}$ for HSC-F cells. Current estimates of viral burst size in the literature rely on inhibiting multiple rounds of infection by antiviral drugs, washouts of infected cells, serial dilutions of infected cells, or infection by single-cycle virus [11,20,21,45,46]. The inhibition of the multiple rounds of infection, however, can introduce additional confounding factors on the viral burst size as discussed in [20]. Here, we have calculated the burst size of SHIV-KS661 in HSC-F cells indirectly by estimating the viral production rate and the average lifespan of infected cells over the course of a typical infection. Our estimate is quite close to the $\sim 5 \times 10^4$ RNA value determined in recent SIV single-cycle virion experiments *in vivo* [20], which, notably, was 10-100 times higher than most previously measured values. We also calculated a basic reproductive number for SHIV-KS661 in HSC-F cell cultures as approximately *62.8* for the initial stages of the infection and approximately *7.01* for the entire course, when the effects of manual removal of virus and cells are included. The latter value implies that reducing viral growth by about 85.7% for the entire course with antiviral intervention, for example, would prevent viral spread *in vitro* given the daily sampling.

It is widely believed that retroviruses are predominantly defective, with less than 0.1% of virions in plasma or culture media being infectious [47-49]. On the other hand, it has recently been suggested that HIV-1 virions, for example, are inherently highly infectious, but that slow viral diffusion in liquid media and rapid dissociation of virions from cells severely limit infections in cultures (i.e., in assays measuring infectivity) [50,51]. On both sides of this debate, however, studies have often relied on measurements of the proportion of infectious virus in stock samples, or on measurements of the infectious/non-infectious ratio over the course of an *in vitro* experiment. These direct measurements of the infectivity ratio in a virus sample are necessarily confounded by a continuous loss of infectious virus, driven by thermal deactivation and RNA degradation and, as such, these analyses cannot address the question of what fraction of virus are infectious at the time of production. Here, we have estimated the production rates of both infectious and non-infectious virus, allowing for a novel quantitative specification of the fraction of newly generated virus that is infectious. This fundamental quantity is important in understanding the role and influence of defective virus particles [48-50,52]; and, to our knowledge, this has not been measured before for any virus strain. We determined the theoretical minimum value for the proportion of infectious virions among newly produced virus, p, to be 8.62×10^{-6}, by calculating the ratio of the infectious to total viral production rates k_{50}/k. The ratio of the production rates, however, is actually p multiplied by α, where α is the conversion factor from RNA count of infectious virions to $TCID_{50}$ (i.e., roughly the fraction of infectious virions that are actually measured in a $TCID_{50}$ titration assay). Therefore, since α is likely much less than one, the proportion of infectious virus is likely much higher. In fact, using the

measured basic reproductive number, we estimate that the minimum value of p is approximately 2.84×10^{-3}, meaning that at least 1 of every 350 virions produced is infectious. Determining this quantity is particularly important in determining the true efficiency of infectious virus replication. In previous publications [53,54], it was reported that *vif*-deficient HIV-1 showed decreased production of infectious virus due to the inhibition of the viral replication process by host factors such as APOBEC3 protein. Our method suggests a novel and more reliable way to determine the effect of the host-viral protein interaction on infectious viral replication.

In another aspect of viral infectivity, we found that the SHIV-KS661 virion infectious half-life at 37°C was 17.9 h. While this quantity is vital for understanding viral dynamics *in vitro*, and represents an important, strain-specific physical property of the virion, it is unlikely to strongly influence *in vivo* dynamics, due to the extremely high physical clearance rate in the blood (virion half-lives are on the order of minutes) [23].

Conclusions

To conclude, by using a simple mathematical model for SHIV-KS661 infection on HSC-F cells and an abundant, diverse experimental dataset, we have been able to reliably estimate the parameters characterizing cell-virus interactions *in vitro*. Based on these estimated parameters, we have provided a quantitative description of SHIV-KS661 kinetics in HSC-F cell cultures which is consistent with previous studies of lentiviruses and provides a number of novel quantities. Most notably, our analysis provides an estimate of the minimum fraction of infectious virus produced by an infected cell. Our improved method for quantifying viral kinetics *in vitro* - which depends crucially on detailed time-course information about the infection of cells in addition to that of virus (both total particle count and infectious titer) - could be applied to other viral infections. The method could likely improve the understanding of the differences in replication across different strains [25,55] or between complete and protein-deficient viruses [53,54]; the differences in viral pathogenesis [6]; and the effects of anti-viral therapies [9,13]. Quantifying the *in vitro* viral kinetics for viruses such as HCV [56,57], for which a convenient animal experimental model has not been established, is of particular interest. Since the method presented here allows for the complete resolution of all viral kinetic parameters, it also enables the identification of the mechanisms of action for new antiviral compounds. Indeed, repeating the experimental infection under various antiviral concentrations would distinctly reveal which parameters (e.g., half-life of infected cells, infectious viral burst size) are affected by the antiviral and to what extent. Furthermore, the inhibitory concentration of the compound could be independently determined for each parameter. Thus, our synergistic approach, combining experiments and mathematical models, has broad potential applications in virology.

Methods

Virus and cell culture

The virus stock of SHIV-KS661 [5] was prepared in a $CD4^+$ human T lymphoid cell line, M8166 (a subclone of C8166) [58]. The stock was stored in liquid nitrogen until use. Establishment of the HSC-F cell line has been previously described [59]. This is a cynomolgous monkey $CD4^+$ T-cell line from fetal splenocytes that were immortalized by infection with Herpesvirus saimiri subtype C. The cells were cultured in RPMI-1640 medium supplemented with 10% fetal calf serum at 37°C and 5% CO_2 in humidified condition.

In vitro experiment

Each experiment was performed using 2 wells of a 24-well plate with a total suspension volume of 2 ml (1 ml per well) and an initial cell concentration of 6.46×10^6 cells/ml in each well. Because the initial cell concentration is close to the carrying capacity of 24-well plates and the doubling time of HSC-F cells is not short, the population of target cells, in the absence of SHIV-KS661 infection, changes very little on the timescale of our experiment. We therefore neglected the effects of potential regeneration of HSC-F cells when constructing the mathematical model.

Cultures of HSC-F cells were inoculated at different MOIs (2.0×10^{-3}, 2.0×10^{-4}, 2.0×10^{-5}, 2.0×10^{-6}; MOI = TCID50/cell) of SHIV-KS661 and incubated for 4 h at 37°C. After inoculation, cells were washed three times to remove the infection medium and placed in fresh media. Subsequently, the culture supernatant was harvested daily for 9 d, along with a small fraction of the cells (5.5%) for counting of viable and infected cells. The remaining cells were then gently washed three times and placed in a fresh, virus-free, medium. Separate experiments (not shown) determined that free virus was not completely removed, but that virus concentration in the supernatant dropped to 0.066% of its value prior to this sampling and washing procedure. Harvested culture supernatants were frozen and stored at -80°C until they were assayed via RT-PCR and $TCID_{50}$ titration, as described below.

Count of viable and infected cells

Virus infection of the HSC-F cells was measured by FACS analysis using markers for intracellular SIV Nef antigen expression. The counts of total and viable cells were first determined using a cell counting chamber

(Burker-turk, Erma, Tokyo, Japan) with trypan blue staining. Viable HSC-F cells (gated by forward- and side-scatter results) were examined by flow cytometry to measure the intracellular SIV Nef antigen expression (see Figure 4). Cells were permeabilized with detergent-containing buffer (Permeabilizing Solution 2, BD Biosciences, San Jose, CA). The permeabilized cells were stained with anti-SIV Nef monoclonal antibody (04-001, Santa Cruz Biotechnology, Santa Cruz, CA) labeled by Zenon Alexa Fluor 488 (Invitrogen, Carlsbad, CA), and analyzed on FACSCalibur (BD Biosciences, San Jose, CA).

Total and infectious viral load quantification

We followed the kinetics of both the total and infectious SHIV-KS661 viral load. The total viral load was measured with a real-time PCR quantification assay, as described previously [5], with minor modifications. Briefly, total RNA was isolated from the culture supernatants (140 μl) of virus-infected HSC-F cells with a QIAamp Viral RNA Mini kit (QIAGEN, Hilden, Germany). RT reactions and PCR were performed by a QuantiTect probe RT-PCR Kit (QIAGEN, Hilden, Germany) using the following primers for the *gag* region; SIV2-696F (5'-GGA AAT TAC CCA GTA CAA CAA ATAGG-3') and SIV2-784R (5'-TCT ATC AAT TTT ACC CAGGCA TTT A-3'). A labeled probe, SIV2-731T (5'-Fam-TGTCCA CCT GCC ATT AAG CCC G-Tamra-3'), was used for detection of the PCR products. These reactions were performed with a Prism 7500 Sequence Detector (Applied Biosystems, Foster City, CA) and analyzed using the manufacturer's software. For each run, a standard curve was generated from dilutions whose copy numbers were known, and the RNA in the culture supernatant samples was quantified based on the standard curve. The infectious viral load was measured by $TCID_{50}$ assay in HFC-S cell cultures using 96-well flat bottom plates at cell concentrations of 1.0×10^6 cells/ml. The titer of the virus was determined as described by Reed and Muench [60].

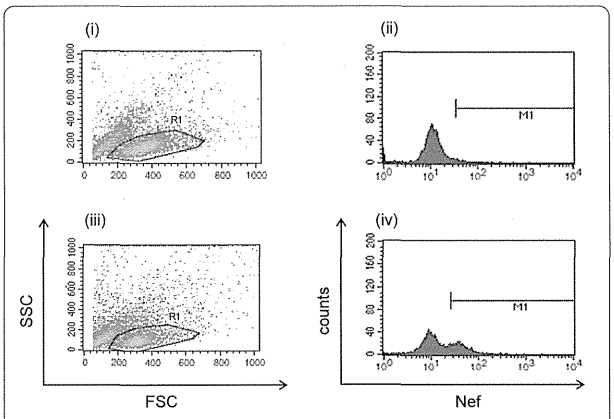

Figure 4 Flow cytometry analysis of HSC-F cells stained with Nef antigen. Representative data at 1 day (i and ii) and 5 days (iii and iv) post-inoculation with SHIV-KS661 at an MOI of 2×10^{-5} are shown. The viable cell population, gated by the data of forward (FSC) and side scatter (SSC) (region surrounded with a solid line in (i) and (iii), respectively), was fractionated by Alexa-488-labeled Nef staining in (ii) and (iv). The counts within the M1 regions and the remaining parts of the total counts are defined as the fraction of Nef- positive (infected) and Nef-negative (target) cells, respectively.

Rate of RNA degradation and loss of infectivity for SHIV-KS661 in the culture condition

The RNA degradation and thermal deactivation of SHIV-KS661 was measured by incubating 4 ml of stock virus, without cells, in a 35 mm Petri dish under the same conditions as the infection experiments (in RPMI-1640 medium supplemented with 10% fetal calf serum at 37°C and 5% CO_2 in humidified condition). Aliquots of the stock (500 μl) were sampled every day from day 0 to day 5 and stored at -80°C (see Figure 2). The RNA copy number and 50% tissue culture infectious dose of the samples were measured as described above.

Mathematical model and fitting

We simultaneously fit Eqs.(5)-(8) to the concentration of Nef-negative and Nef-positive HSC-F cells and the infectious and total viral loads at four different MOIs (Figure 3) using nonlinear least-squares regression (FindMinimum package of *Mathematica7.0*) which minimizes the following objective function:

$$SSR = \sum_{j=1}^{4}\left[\sum_{i=1}^{9}\left\{\log x_j(t_i) - \log x_j^e(t_i)\right\}^2 + \sum_{i=1}^{9}\left\{\log y_j(t_i) - \log y_j^e(t_i)\right\}^2 + \sum_{i=1}^{9}\left\{\log v_{RNAj}(t_i) - \log v_{RNAj}^e(t_i)\right\}^2 + \sum_{i=1}^{9}\left\{\log v_{50j}(t_i) - \log v_{50j}^e(t_i)\right\}^2\right]$$

where $x_j(t_i)$, $y_j(t_i)$, $v_{RNAj}(t_i)$, and $v_{50j}(t_i)$ are the model-predicted values for Nef-negative cells, Nef-positive cells, total RNA viral load and infectious ($TCID_{50}$) viral load, given by the solution of Eqs.(5)-(8) at measurement time t_i (t_i = 0, 1, 2, ..., 8 d). Index j is a label for the MOI of the four experiments (i.e., for MOI: 2.0×10^{-3}, 2.0×10^{-4}, 2.0×10^{-5}, and 2.0×10^{-6}). The variables with superscript "e" are the corresponding experimental measurements of those quantities. Note that the HSC-F cells were inoculated with SHIV-KS661 24 h before t = 0. Experimental measurements below the detection limit (marked "d.l." in Table 1) were excluded when computing the *SSR*. Alternative fits with various weights on the infectious viral load to account for larger errors in the $TCID_{50}$ value [61], were also performed, but these did not significantly alter the extracted parameter values (Additional files 4, 5, 6, 7, 8, 9). To derive the 95% confidence interval for each parameter, we employed the

bootstrap method [62,63], estimating parameter values using 256 replicates of the four data sets and calculating the 2.5 and 97.5 percentiles.

Additional material

Additional file 1: Fit of a mathematical model which includes an eclipse phase of infection to experimental data of SHIV-KS661 *in vitro*. Testing a variant of the model which incorporates an "eclipse" phase of infection to represent the cell's period of latency prior to virus production (see Additional file 2 for more detailed information).

Additional file 2: Additional documentation for Additional files 1. Detailed explanation of mathematical models used in Additional files 1.

Additional file 3: Table for estimated parameters in Additional files 1. Parameters values, initial values and derived quantities for the *in vitro* experiment with eclipse model.

Additional file 4: Fit of the mathematical model with SSR^W (W = 0.0001) to experimental data of SHIV-KS661 *in vitro* (a). Fitting with weight of $W = 0.0001$ on the infectious viral load to account for larger errors in the $TCID_{50}$ value (see Additional file 8 for more detailed information).

Additional file 5: Fit of the mathematical model with SSR^W (W = 0.1) to experimental data of SHIV-KS661 *in vitro* (b). Fitting with weight of $W = 0.1$ on the infectious viral load to account for larger errors in the $TCID_{50}$ value (see Additional file 8 for more detailed information).

Additional file 6: Fit of the mathematical model with SSR^W (W = 10) to experimental data of SHIV-KS661 *in vitro* (c). Fitting with weight of $W = 10$ on the infectious viral load to account for larger errors in the $TCID_{50}$ value (see Additional file 8 for more detailed information).

Additional file 7: Fit of the mathematical model with SSR^W (W = 10000) to experimental data of SHIV-KS661 *in vitro* (d). Fitting with weight of $W = 10000$ on the infectious viral load to account for larger errors in the $TCID_{50}$ value (see Additional file 8 for more detailed information).

Additional file 8: Additional documentation for Additional files 4, 5, 6, 7. Detailed explanation of mathematical models used in **Additional files** 4, 5, 6, 7.

Additional file 9: Table for estimated parameters in Additional files 4, 5, 6, 7. Parameters values and derived quantities for the *in vitro* experiment with various SSR^Ws.

List of abbreviations

SHIV: simian/human immunodeficiency virus; HIV-1: human immunodeficiency virus type-1; MDCK: Madin Darby canine kidney; HF: hollow-fiber; IC_{50}: 50% inhibitory concentration; HCV: hepatitis C virus; HA: hemagglutination assay; $TCID_{50}$: 50% tissue culture infection dose; PFU: plaque forming units; MOI: multiplicities of infection; PB: peripheral blood.

Acknowledgements

This work was supported, in part, by JST PRESTO program (SI) and by the Natural Sciences and Engineering Research Council of Canada (CAAB) and by a grant-in-aid for scientific research from the Ministry of Education and Science, Japan, Research on Human Immunodeficiency Virus/AIDS in Health and Labor Sciences research grants from the Ministry of Health, Labor and Welfare, Japan, a research grant for health sciences focusing on drug innovation for AIDS from the Japan Health Sciences Foundation (TM).

Author details

[1]Precursory Research for Embryonic Science and Technology (PRESTO), Japan Science and Technology Agency (JST), Kawaguchi, Saitama 332-0012, Japan. [2]Graduate School of Mathematical Sciences, The University of Tokyo, Meguro-ku, Tokyo 153-8914, Japan. [3]Institute for Virus Research, Kyoto University, Kyoto, Kyoto 606-8507, Japan. [4]Department of Physics, Ryerson University, ON, Toronto M5B 2K3, Canada. [5]Department of Systems Engineering, Shizuoka University, Hamamatsu, Shizuoka 432-8561, Japan. [6]Department of Biology, Faculty of Sciences, Kyushu University, 6-10-1 Hakozaki, Higashi-ku, Fukuoka, Fukuoka 812-8581, Japan.

Authors' contributions

SI, KS, TI and TM designed the study.
SI, BPH and SM carried out data analysis.
TT and TM performed all experiments.
SI and CAAB developed mathematical model.
SI, BPH, CAAB and TM wrote the final manuscript.
All authors read and approved the final manuscript.

Competing interests

The authors declare that they have no competing interests.

Received: 7 October 2011 Accepted: 25 February 2012
Published: 25 February 2012

References

1. Harouse JM, Gettie A, Tan RC, Blanchard J, Cheng-Mayer C: **Distinct pathogenic sequela in rhesus macaques infected with CCR5 or CXCR4 utilizing SHIVs.** *Science* 1999, **284**:816-819.
2. Matsuda K, Inaba K, Fukazawa Y, Matsuyama M, Ibuki K, Horiike M, Saito N, Hayami M, Igarashi T, Miura T: ***In vivo* analysis of a new R5 tropic SHIV generated from the highly pathogenic SHIV-KS661, a derivative of SHIV-89.6.** *Virology* 2010, **399**:134-143.
3. Nishimura Y, Igarashi T, Donau OK, Buckler-White A, Buckler C, Lafont BA, Goeken RM, Goldstein S, Hirsch VM, Martin MA: **Highly pathogenic SHIVs and SIVs target different $CD4^+$ T cell subsets in rhesus monkeys explaining their divergent clinical courses.** *Proc Natl Acad Sci USA* 2004, **101**:12324-12329.
4. Reimann KA, Li JT, Veazey R, Halloran M, Park IW, Karlsson GB, Sodroski J, Letvin NL: **A chimeric simian/human immunodeficiency virus expressing a primary patient human immunodeficiency virus type 1 isolate env causes an AIDS-like disease after in vivo passage in rhesus monkeys.** *J Virol* 1996, **70**:6922-6928.
5. Shinohara K, Sakai K, Ando S, Ami Y, Yoshino N, Takahashi E, Someya K, Suzaki Y, Nakasone T, Sasaki Y, Kaizu M, Lu Y, Honda M: **A highly pathogenic simian/human immunodeficiency virus with genetic changes in cynomolgus monkey.** *J Gen Virol* 1999, **80**:1231-1240.
6. Kozyrev IL, Ibuki K, Shimada T, Kuwata T, Takemura T, Hayami M, Miura T: **Characterization of less pathogenic infectious molecular clones derived from acute-pathogenic SHIV-89.6p stock virus.** *Virology* 2001, **282**:6-13.
7. Miyake A, Ibuki K, Enose Y, Suzuki H, Horiuchi R, Motohara M, Saito N, Nakasone T, Honda M, Watanabe T, Miura T, Hayami M: **Rapid dissemination of a pathogenic simian/human immunodeficiency virus to systemic organs and active replication in lymphoid tissues following intrarectal infection.** *J Gen Virol* 2006, **13**:11-20.
8. Inaba K, Fukazawa Y, Matsuda K, Himeno A, Matsuyama M, Ibuki K, Miura Y, Koyanagi Y, Nakajima A, Blumberg RS, Takahashi H, Hayami M, Igarashi T, Miura T: **Small intestine $CD4^+$ cell reduction and enteropathy in simian/human immunodeficiency virus KS661-infected rhesus macaques in the presence of low viral load.** *J Gen Virol* 2010, **91**:773-781.
9. Dixit NM, Layden-Almer JE, Layden TJ, Perelson AS: **Modelling how ribavirin improves interferon response rates in hepatitis C virus infection.** *Nature* 2004, **432**:922-924.
10. Ho DD, Neumann AU, Perelson AS, Chen W, Leonard JM, Markowitz M: **Rapid turnover of plasma virions and CD4 lymphocytes in HIV-1 infection.** *Nature* 1995, **373**:123-126.
11. Little SJ, McLean AR, Spina CA, Richman DD, Havlir DV: **Viral dynamics of acute HIV-1 infection.** *J Exp Med* 1999, **190**:841-850.
12. Markowitz M, Louie M, Hurley A, Sun E, Di Mascio M, Perelson AS, Ho DD: **A novel antiviral intervention results in more accurate assessment of human immunodeficiency virus type 1 replication dynamics and T-cell decay in vivo.** *J Virol* 2003, **77**:5037-5038.
13. Neumann AU, Lam NP, Dahari H, Gretch DR, Wiley TE, Layden TJ, Perelson AS: **Hepatitis C viral dynamics in vivo and the antiviral efficacy of interferon-alpha therapy.** *Science* 1998, **282**:103-107.
14. Perelson AS, Essunger P, Cao Y, Vesanen M, Hurley A, Saksela K, Markowitz M, Ho DD: **Decay characteristics of HIV-1-infected compartments during combination therapy.** *Nature* 1997, **387**:188-191.

15. Perelson AS, Neumann AU, Markowitz M, Leonard JM, Ho DD: **HIV-1 dynamics in vivo: virion clearance rate, infected cell life-span, and viral generation time.** *Science* 1996, **271**:1582-1586.
16. Ribeiro RM, Qin L, Chavez LL, Li D, Self SG, Perelson AS: **Estimation of the initial viral growth rate and basic reproductive number during acute HIV-1 infection.** *J Virol* 2010, **84**:6096-6102.
17. Stafford MA, Corey L, Cao Y, Daar ES, Ho DD, Perelson AS: **Modeling plasma virus concentration during primary HIV infection.** *J Theor Biol* 2000, **203**:285-301.
18. Baccam P, Beauchemin C, Macken CA, Hayden FG, Perelson AS: **Kinetics of influenza A virus infection in humans.** *J Virol* 2006, **80**:7590-7599.
19. Beauchemin CA, McSharry JJ, Drusano GL, Nguyen JT, Went GT, Ribeiro RM, Perelson AS: **Modeling amantadine treatment of influenza A virus *in vitro*.** *J Theor Biol* 2008, **254**:439-451.
20. Chen HY, Di Mascio M, Perelson AS, Ho DD, Zhang L: **Determination of virus burst size in vivo using a single-cycle SIV in rhesus macaques.** *Proc Natl Acad Sci USA* 2007, **104**:19079-19084.
21. Dimitrov DS, Willey RL, Sato H, Chang LJ, Blumenthal R, Martin MA: **Quantitation of human immunodeficiency virus type 1 infection kinetics.** *J Virol* 1993, **67**:2182-2190.
22. Dinoso JB, Rabi SA, Blankson JN, Gama L, Mankowski JL, Siliciano RF, Zink MC, Clements JE: **A simian immunodeficiency virus-infected macaque model to study viral reservoirs that persist during highly active antiretroviral therapy.** *J Virol* 2009, **83**:9247-9257.
23. Igarashi T, Brown C, Azadegan A, Haigwood N, Dimitrov D, Martin MA, Shibata R: **Human immunodeficiency virus type 1 neutralizing antibodies accelerate clearance of cell-free virions from blood plasma.** *Nat Med* 1999, **5**:211-216.
24. Miao H, Hollenbaugh JA, Zand MS, Holden-Wiltse J, Mosmann TR, Perelson AS, Wu H, Topham DJ: **Quantifying the early immune response and adaptive immune response kinetics in mice infected with influenza A virus.** *J Virol* 2010, **84**:6687-6698.
25. Mitchell H, Levin D, Forrest S, Beauchemin CA, Tipper J, Knight J, Donart N, Layton RC, Pyles J, Gao P, Harrod KS, Perelson AS, Koster F: **Higher level of replication efficiency of 2009 (H1N1) pandemic influenza virus than those of seasonal and avian strains: kinetics from epithelial cell culture and computational modeling.** *J Virol* 2011, **85**:1125-1135.
26. Mohler L, Flockerzi D, Sann H, Reichl U: **Mathematical model of influenza A virus production in large-scale microcarrier culture.** *Biotechnol Bioeng* 2005, **90**:46-58.
27. Nowak MA, Lloyd AL, Vasquez GM, Wiltrout TA, Wahl LM, Bischofberger N, Williams J, Kinter A, Fauci AS, Hirsch VM, Lifson JD: **Viral dynamics of primary viremia and antiretroviral therapy in simian immunodeficiency virus infection.** *J Virol* 1997, **71**:7518-7525.
28. Regoes RR, Barber DL, Ahmed R, Antia R: **Estimation of the rate of killing by cytotoxic T lymphocytes in vivo.** *Proc Natl Acad Sci USA* 2007, **104**:1599-1603.
29. Schulze-Horsel J, Schulze M, Agalaridis G, Genzel Y, Reichl U: **Infection dynamics and virus-induced apoptosis in cell culture-based influenza vaccine production - Flow cytometry and mathematical modeling.** *Vaccine* 2009, **27**:2712-2722.
30. Funk GA, Fischer M, Joos B, Opravil M, Gunthard H, Huldrych F, Ledergerber B, Bonhoeffer S: **Quantification of In Vivo Replicative Capacity of HIV-1 in Different Compartments of Infected Cells.** *JAIDS* 2001, **26**:397-404.
31. Hlavacek WS, Stilianakis NI, Notermans DW, Danner SA, Perelson AS: **Influence of follicular dendritic cells on decay of HIV during antiretroviral therapy.** *Proc Natl Acad Sci USA* 2000, **97**:10966-10971.
32. Kepler GM, Nguyen HK, Webster-Cyriaque J, Banks HT: **A dynamic model for induced reactivation of latent virus.** *J Theor Biol* 2007, **244**:451-462.
33. Murray JM, Purcell RH, Wieland SF: **The half-life of hepatitis B virions.** *Hepatology* 2006, **44**:1117-1121.
34. Regoes RR, Antia R, Garber DA, Silvestri G, Feinberg MB, Staprans SI: **Roles of target cells and virus-specific cellular immunity in primary simian immunodeficiency virus infection.** *J Virol* 2004, **78**:4866-4875.
35. Speirs C, van Nimwegen E, Bolton D, Zavolan M, Duvall M, Angleman S, Siegel R, Perelson AS, Lenardo MJ: **Analysis of human immunodeficiency virus cytopathicity by using a new method for quantitating viral dynamics in cell culture.** *J Virol* 2005, **79**:4025-4032.
36. Stilianakis NI, Boucher CAB, deJong MD, van Leeuwen R, Schuurman R, de Boer RJ: **Clinical data sets of HIV1 Reverse transcriptase-resistant mutants explained by a mathematical model.** *J Virol* 1997, **71**:161-168.
37. Verotta D, Schaedeli F: **Non-linear dynamics modes characterizing long-term virological data from AIDS clinical trials.** *Math Biosci* 2002, **176**:163-183.
38. Nowak MA, May RM: **Virus dynamics.** Oxford University Press; 2000.
39. Perelson AS: **Modeling viral and immune system dynamics.** *Nat Rev Immunol* 2001, **2**:28-36.
40. Bangham CRM, Kirkwood TBL: **Defective interfering particles: Effects in modulating virus growth and persistence.** *Virology* 1990, **179**:821-826.
41. Ma ZM, Stone M, Piatak M, Schweighardt B, Haigwood NL, Montefiori D, Lifson JD, Busch MP, Miller CJ: **High specific infectivity of plasma virus from the pre-ramp-up and ramp-up stages of acute Simian Immunodeficiency Virus infection.** *J Virol* 2009, **83**:3288-3297.
42. Vaidya NK, Ribeiro RM, Miller CJ, Perelson AS: **Viral dynamics during primary Simian Immunodeficiency Virus Infection: Effect of Time-dependent Virus Infectivity.** *J Virol* 2010, **84**:4302-4310.
43. Anderson RM: **The Kermack-McKendrick Epidemic Threshold Theorem.** *Bull Math Biol* 1991, **53**:3-32.
44. Brandin E, Thorstensson R, Bonhoeffer S, Albert J: **Rapid viral decay in simian immunodeficiency virus-infected macaques receiving quadruple antiretroviral therapy.** *J Virol* 2006, **80**:9861-9864.
45. Eckstein DA, Penn ML, Korin YD, Scripture-Adams DD, Zack JA, Kreisberg JF, Roederer M, Sherman MP, Chin PS, Goldsmith MA: **HIV-1 actively replicates in naive CD4(+) T cells residing within human lymphoid tissues.** *Immunity* 2001, **15**:671-682.
46. Tsai WP, Conley SR, Kung HF, Garrity RR, Nara PL: **Preliminary in vitro growth cycle and transmission studies of HIV-1 in an autologous primary cell assay of blood-derived macrophages and peripheral blood mononuclear cells.** *Virology* 1996, **226**:205-216.
47. Huang AS, Baltimore D: **Defective viral particles and viral disease processes.** *Nature* 1970, **226**:325-327.
48. Kwon YJ, Hung G, Anderson WF, Peng CA, Yu H: **Determination of infectious retrovirus concentration from colony-forming assay with quantitative analysis.** *J Virol* 2003, **77**:5712-5720.
49. Rusert P, Fischer M, Joos B, Leemann C, Kuster H, Flepp M, Bonhoeffer S, Gunthard HF, Trkola A: **Quantification of infectious HIV-1 plasma viral load using a boosted in vitro infection protocol.** *Virology* 2004, **326**:113-129.
50. Platt EJ, Kozak SL, Durnin JP, Hope TJ, Kabat D: **Rapid dissociation of HIV-1 from cultured cells severely limits infectivity assays, causes the inactivation ascribed to entry inhibitors, and masks the inherently high level of infectivity of virions.** *J Virol* 2010, **84**:3106-3110.
51. Thomas JA, Ott DE, Gorelick RJ: **Efficiency of Human Immunodeficiency Virus Type 1 Postentry Infection Processes: Evidence against Disproportionate Numbers of Defective Virions.** *J Virol* 2007, **81**:4367-4370.
52. Marcus PI, Ngunjiri JM, Sekellick MJ: **Dynamics of biologically active subpopulations of influenza virus: Plaque-forming, noninfectious cell-killing, and defective interfering particles.** *J Virol* 2009, **83**:8122-8130.
53. Izumi T, Io K, Matsui M, Shirakawa K, Shinohara M, Nagai Y, Kawahara M, Kobayashi M, Kondoh H, Misawa N, Koyanagi Y, Uchiyama T, Takaori-Kondo A: **HIV-1 viral infectivity factor interacts with TP53 to induce G2 cell cycle arrest and positively regulate viral replication.** *Proc Natl Acad Sci USA* 2010, **107**:20798-20803.
54. Sato K, Izumi T, Misawa N, Kobayashi T, Yamashita Y, Ohmichi M, Ito M, Takaori-Kondo A, Koyanagi Y: **Remarkable lethal G-to-A mutations in vif-proficient HIV-1 provirus by individual APOBEC3 proteins in humanized mice.** *J Virol* 2010, **84**:9546-9556.
55. De Jong MD, Simmons CP, Thanh TT, Hien VM, Smith GJD, Chau TNB, Hoang DM, Chau NVV, Khanh TH, Dong VC, Qui PT, Cam BV, Ha DQ, Guan Y, Peiris JSM, Chinh NT, Hien TT, Farrar J: **Fatal outcome of human influenza A (H5N1) is associated with high viral load and hypercytokinemia.** *Nat Med* 2006, **12**:1203-1207.
56. Wakita T, Pietschmann T, Kato T, Date T, Miyamoto M, Zhao Z, Murthy K, Habermann A, Kräusslich HG, Mizokami M, Bartenschlager R, Liang TJ: **Production of infectious hepatitis C virus in tissue culture from a cloned viral genome.** *Nat Med* 2005, **11**:791-796.
57. Watashi K, Ishii N, Hijikata M, Inoue D, Murata T, Miyanari Y, Shimotohno K: **Cyclophilin B is a functional regulator of hepatitis C virus RNA polymerase.** *Mol Cell* 2005, **19**:111-122.

58. Clapham PR, Weiss RA, Dalgleish AG, Exley M, Whitby D, Hogg N: **Human immunodeficiency virus infection of monocytic and T-lymphocytic cells: receptor modulation and differentiation induced by phorbol ester.** *Virology* 1987, **158**:44-51.
59. Akari H, Mori K, Terao K, Otani I, Fukasawa M, Mukai R, Yoshikawa Y: ***In vitro* immortalization of Old World monkey T lymphocytes with Herpesvirus saimiri: its susceptibility to infection with simian immunodeficiency viruses.** *Virology* 1996, **218**:382-388.
60. Reed LJ, Muench H: **A simple method of estimating fifty per cent endpoints.** *Am J Hyg* 1938, **27**:493-497.
61. Macken C: **Design and analysis of serial limiting dilution assays with small sample sizes.** *J Immunol Methods* 1999, **222**:13-29.
62. Efron B: **Bootstrap Method: Another Look at the Jackknife.** *Annals of Statistic* 1979, **7**:1-26.
63. Efron B, Tibshirani R: **Bootstrap methods for standard errors, confidence intervals, and other measures of statistical accuracy.** *Stat Sci* 1986, **1**:54-75.

doi:10.1186/PREACCEPT-8502330256154242
Cite this article as: Iwami *et al.*: Quantification system for the viral dynamics of a highly pathogenic simian/human immunodeficiency virus based on an *in vitro* experiment and a mathematical model. *Retrovirology* 2012 **9**:18.

Biochemical and Biophysical Research Communications 421 (2012) 291–295

Contents lists available at SciVerse ScienceDirect

Biochemical and Biophysical Research Communications

journal homepage: www.elsevier.com/locate/ybbrc

Minor contribution of HLA class I-associated selective pressure to the variability of HIV-1 accessory protein Vpu

Zafrul Hasan [a], Jonathan M. Carlson [b], Hiroyuki Gatanaga [a,c], Anh Q. Le [d], Chanson J. Brumme [e], Shinichi Oka [a,c], Zabrina L. Brumme [d,e], Takamasa Ueno [a,*]

[a] Center for AIDS Research, Kumamoto University, Japan
[b] Microsoft Research, Los Angeles, CA, USA
[c] AIDS Clinical Center, National Center for Global Health and Medicine, Japan
[d] Simon Fraser University, Burnaby, BC, Canada
[e] BC Center for Excellence in HIV/AIDS, Vancouver, BC, Canada

ARTICLE INFO

Article history:
Received 17 March 2012
Available online 7 April 2012

Keywords:
HIV/AIDS
Vpu
HLA class I
Viral evolution

ABSTRACT

Host HLA class I (HLA-I) allele-associated immune responses are major forces driving the evolution of HIV-1 proteins such as Gag and Nef. The viral protein U (Vpu) is an HIV-1 accessory protein responsible for CD4 degradation and enhancement of virion release by antagonizing tetherin/CD317. Although Vpu represents one of the most variable proteins in the HIV-1 proteome, it is still not clear to what extent HLA-I influence its evolution. To examine this issue, we enrolled 240 HLA-I-typed, treatment naïve, chronically HIV-infected subjects in Japan, and analyzed plasma HIV RNA nucleotide sequences of the vpu region. Using a phylogenetically-informed method incorporating corrections for HIV codon covariation and linkage disequilibrium among HLA alleles, we investigated HLA-associated amino acid mutations in the Vpu protein as well as in the translational products encoded by alternative reading frames. Despite substantial amino acid variability in Vpu, we identified only 4 HLA-associations in all possible translational products encoded in this region, suggesting that HLA-associated immune responses had minor effects on Vpu variability in this cohort. Rather, despite its size (81 amino acids), Vpu showed 103 codon–codon covariation associations, suggesting that Vpu conformation and function are preserved through many possible combinations of primary and secondary polymorphisms. Taken together, our study suggests that Vpu has been comparably less influenced by HLA-I-associated immune-driven evolution at the population level compared to other highly variable HIV-1 accessory proteins.

1. Introduction

Immune-mediated adaptation occurs during an HIV-1 infection. The HLA class I (HLA-I)-restricted $CD8^+$ cytotoxic T lymphocyte (CTL) response is one of the major forces driving HIV evolution, resulting in the selection of CTL escape mutants [1,2]. Despite the extensive genetic diversity of both HIV-1 and HLA-I alleles, escape pathways are reproducible and broadly predictable based on host HLA-I alleles [3–6]. Moreover, analysis of linked HLA-I and HIV datasets from large cohorts of HIV-infected subjects has facilitated our ability to map the landscape of immune escape mutations across HIV-1, identify immunogenic regions, and identify novel CTL epitopes [3,7].

Viral protein U (Vpu) is an accessory protein that is unique to HIV-1 and a subset of related simian immunodeficiency viruses. The HIV-1 Vpu protein has two major functions: degradation of newly synthesized CD4 molecules in the endoplasmic reticulum and enhancement of the release of progeny virions from infected cells by antagonizing tetherin/CD317, a host restriction factor that directly binds and retains viral particles on the surface of infected cells (reviewed in [8,9]). As such, Vpu is thought to play a role in virus spread and pathogenesis *in vivo*. Interestingly, Vpu is the most variable protein among all HIV proteins as evidenced by a cross-sectional comparison of HIV-1 sequences isolated from HIV-infected individuals [10], raising the possibility that Vpu undergoes adaptation in response to host immune responses. However, Vpu has been shown to be a minor target for CTLs as revealed by IFN-γ Elispot assays with overlapping peptides based on the subtype B consensus sequence [11]. Considering the highly variable nature of Vpu, it is possible to miss responses if the autologous virus sequence is markedly different from the peptide sequence when using this Elispot assay system [12].

In the present study, we sought to identify HLA-associated polymorphisms in Vpu and alternate reading frames and examine to

* Corresponding author. Address: Center for AIDS Research, Kumamoto University, 2-2-1 Honjo, Kumamoto 860-0811, Japan. Fax: +81 96 373 6825.
E-mail address: uenotaka@kumamoto-u.ac.jp (T. Ueno).

0006-291X/$ - see front matter © 2012 Elsevier Inc. All rights reserved.
http://dx.doi.org/10.1016/j.bbrc.2012.04.002

what extent they are involved in Vpu amino acid variability at the population level. We utilize a published phylogenetic dependency network model [13], a comprehensive evolutionary model that considers all important confounding effects such as HIV phylogeny, HIV codon covariation, and linkage disequilibrium of HLA alleles.

2. Materials and methods

2.1. Patient samples

A total of 240 chronically HIV-1-infected, treatment-naïve subjects (CD4, median 237; IQR, 160-397; viral load, median 33,200; IQR, 222,000-55,400) followed at the AIDS Clinical Center, International Medical Center of Japan were enrolled in this study. All participants provided written informed consent. HLA-I typing was performed as previously described [14]. The most frequently observed *HLA-A, B,* and *C* alleles in this cohort were *HLA-A*24:02*, *HLA-B*52:01*, and *HLA-C*01:02*, respectively, consistent with HLA class I allelic frequencies of the Japanese people [14].

2.2. Sequence analysis of vpu

HIV-1 particles were precipitated by ultracentrifugation (50,000 rpm, 15 min) of patients' plasma, after which the viral RNA was extracted using standard methods. Following reverse transcription, DNA fragments encoding Vpu proteins were amplified by nested PCR, and gel purified as previously described [15,16]. The primers used were as follows: the primers for the first round of amplification were VVVa-F (5′-TTAAAAGAAAAGGGGG GATTGGGGG-3′) and VVVb-R (5′-ATTCCATGTGTACATT GTACTGT-3′); and those for the second round, VVVc-F (5′-AGATAATAGTGAC ATAAAAGTAGTGCCAAGAAG-3′) and VVVd-R (5′-CCATAATAGACT GTGACCCACAA-3′). The *vpu* sequence was then directly analyzed with an automated sequencer (Applied Biosystems 3500xL) and aligned to the *vpu* sequence of the HIV-1 subtype B reference strain HXB2 (Accession No. K03455). More than 90% of the subjects were infected with subtype B, as determined by phylogenetic analysis of concatenated sequences of *vif*, *vpr*, and *vpu* reading frames.

2.3. Analysis of amino acid sequence variability

A Shannon entropy score for each position in the Vpu protein was calculated and used to analyze amino-acid sequence variability, as described previously [10]. Entropy is a measure of the amino acid variability at a given position that takes into account both the number of possible amino acid residues allowed and their frequency.

2.4. Analysis of association between Vpu sequence polymorphisms and host HLA class I alleles

To identify HIV-HLA polymorphism associations, we employed a phylogenetically dependency network model [13], which comprehensively includes all confounding effects of the analysis, such as HIV founder effects, HIV codon co-variation, and linkage disequilibrium of HLA-I alleles. Multiple comparisons are addressed using q-values (refer the detailed methods given in refs. [4,5,13]); in the present study, a cutoff of $q < 0.2$ was used to denote statistically significant associations. HLA-associated polymorphisms were classified into two categories. "Nonadapted" amino acids are enriched in the absence of the restricting HLA of interest. Usually, "nonadapted" forms represent the consensus amino acid at that position, and they can be thought of as the "wild-type" or "susceptible" form particular to that allele. Conversely, "adapted" amino acids are those enriched in the presence of the HLA allele; these can be thought of as the escape variant particular to that allele.

3. Results and discussion

3.1. Genetic variability of the vpu gene

We successfully amplified DNAs encompassing the *vpu* region from 216 of 240 samples (90%). Firstly, we analyzed the amino acid variability at each codon of Vpu by determining its Shannon entropy score. Two amino acid residues, Trp23 and Arg49, showed highly conserved (>98%) among individual sequences. Instead, most codons displayed substantial variability, with the average of the entropy score reaching 0.58 (Fig. 1A), confirming the findings by Yusim et al., which showed that Vpu is a highly variable protein [10]. Also, the amino acid variability of each codon in the present study correlated strongly with that of published subtype B sequence data from the Los Alamos database (Fig. 1B), suggesting that our observed pattern of amino acid variation in Vpu was generally representative of the variation observed in HIV-1 subtype B. In fact, the consensus amino acid sequences of subtype B and the present dataset were identical except for 3 amino-acid residues: positions 3, 5, and 24 (Fig. 1C). These amino acid residues were highly variable (Fig. 1A) and not directly associated with known Vpu functions (Fig. 1C).

3.2. HLA-associated polymorphisms in Vpu

As HLA-I-mediated selective contributes to HIV-1 sequence variability, especially the accessory protein Nef [4], we sought to examine whether HLA-I-mediated selective pressure substantially influenced the evolution of Vpu, another accessory protein. We applied a phylogenetic dependency network model [13], which adjusts for the confounding effects of HIV phylogeny, HIV codon covariation and linkage disequilibrium of HLA-I alleles.

In our dataset of 216 individuals, we identified only three HIV-HLA associations in Vpu: a nonadapted association between C*03 and Glu-5, a nonadapted association between A*33:03 and Arg-37, and an adapted association between A*33:03 and Lys-37. The presence of both nonadapted and adapted A*33:03-associated polymorphisms at Vpu codon 37 is consistent with an Arginine-to-Lysine escape mutation occurring at the C-terminus of the immunodominant HLA-A*33:03-restricted epitope in Vpu, ^{29}EYRKILRQR^{37} [11]. However, there was no HLA-restricted T cell epitopes around Vpu position 5 have been reported. Although we might have missed some polymorphisms due to the limited sample size in this study, these data suggest that HLA-I-mediated selective pressure toward Vpu does not substantially drive Vpu variability at the population level in this cohort.

3.3. HLA-associated polymorphisms in alternating reading frames

CTLs can recognize epitopes encoded by alternate reading frames including the antisense-strand sequences of HIV-1 *gag*, *pol*, and *nef* [17,18]. Therefore, we also investigated HIV-HLA polymorphism associations in peptide sequences encoded by alternative reading frames of the *vpu* gene. We observed no statistically significant HLA-associated polymorphisms in alternate or antisense reading frames, except for a single HLA-B*40:01 associated "adapted" lysine polymorphism at codon 2 of the overlapping Envelope reading frame which is initiated in the middle of the *vpu* gene (ORF + 2; Table 1, Fig. 2). Although this association was between Lys-2 of Env and *HLA-B*40:01*, no CTL epitopes have been reported in the context of HLA-B*40:01 in this region. Using bioinformatic prediction programs Epipred [19] and BIMAS [20] we

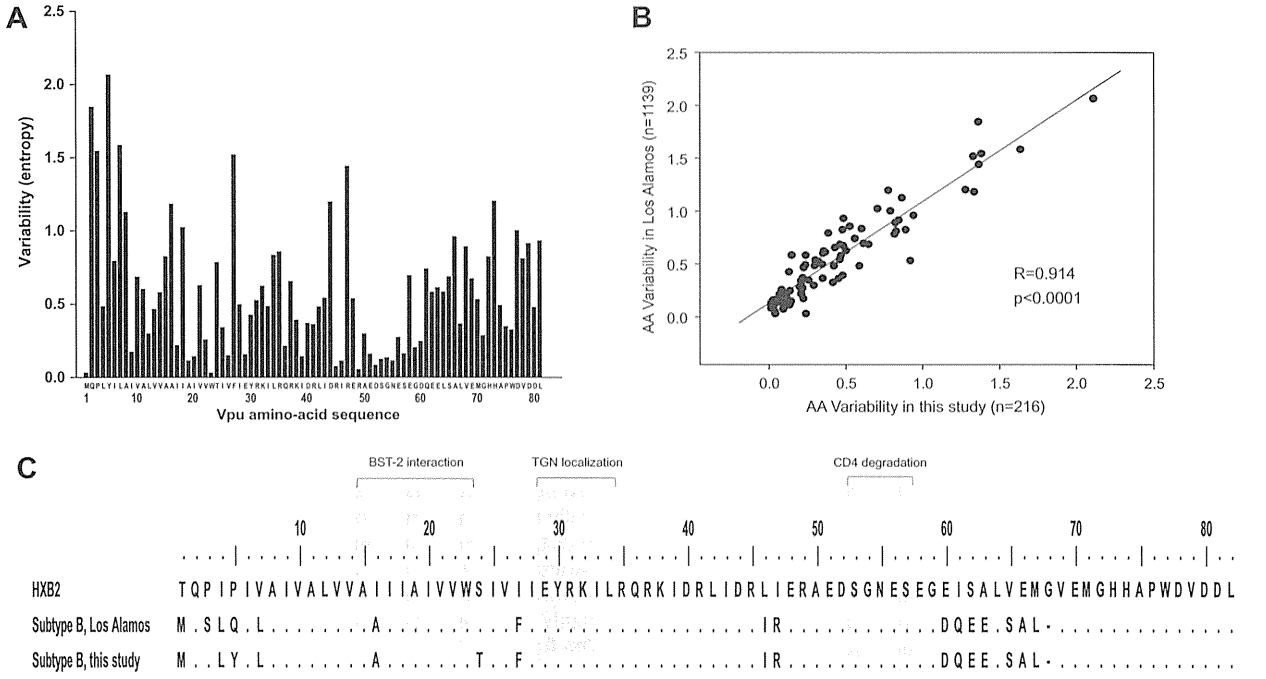

Fig. 1. Variability of the amino acid residues of HIV-1 Vpu. The amino acid sequence of Vpu was analyzed based on the cross-sectional studies on 216 HIV-infected subjects. The amino acid variability at each position of Vpu was analyzed by determining its Shannon entropy score (panel A). The Vpu sequence (subtype B, $n = 1139$) was retrieved from the Los Alamos HIV sequence database, analyzed for its amino acid variability, and compared with subtype B obtained from this study using Spearman Rank Order Correlation (panel B). The consensus sequences of Vpu obtained from Los Alamos database and this study were aligned with reference strain HXB2 and regions responsible for some key Vpu functions highlighted (panel C).

Table 1
Summary of HIV-HLA associations in the Vpu-encoded region.

RF	Protein	Pos HXB2	aa	HLA	Association	*p*-Value	*q*-Value	Known epitope	
								Sequence	Reference
+1	Vpu	5	E	C*03	Nonadapted	2.13×10^{-5}	1.52×10^{-1}	none	–
		37	R	A*22:03	Nonadapted	3.40×10^{-6}	5.50×10^{-2}	^{29}EYRKILRQR^{37}	[11]
		37	K	A*33:03	Adapted	2.80×10^{-5}	1.52×10^{-1}	^{29}EYRKILRQR^{37}	[11]
+2	Env	2	K	B*40:01	Adapted	1.63×10^{-5}	1.67×10^{-1}	none	–

RF, reading frame; Pos HXB2, amino acid position when aligned to HXB2 sequence.

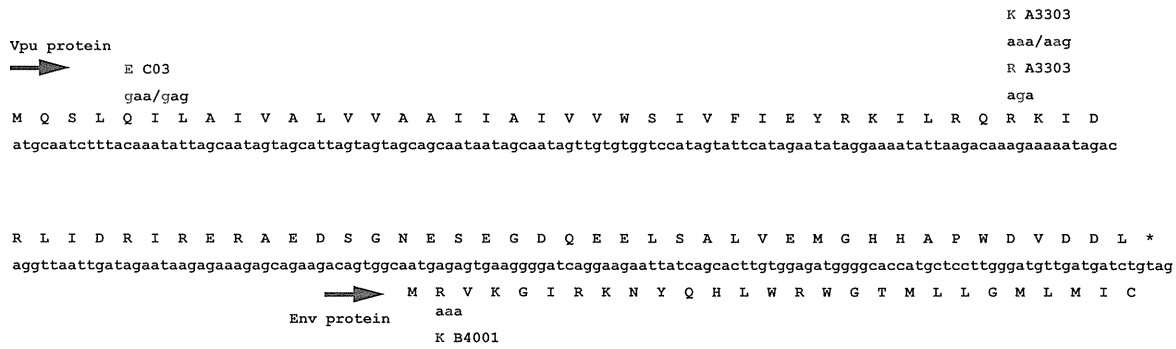

Fig. 2. The Vpu and a part of Env proteins and their associations with host HLA class I alleles. The nucleotide sequence and its deduced amino acid sequence of Vpu and of an overlapping part of Env with reference to the subtype B consensus sequence of Los Alamos database is shown. The amino acid residues associated with the indicated HLA class I alleles ($p < 0.05$, $q < 0.2$) are shown with adapted (red) and nonadapted (blue) residues. (For interpretation of the references to colour in this figure legend, the reader is referred to the web version of this article.)

attempted to predict B*40:01-restricted CTL epitopes, but found none (data not shown). This failure is most likely due to the presence of several basic amino acids, such as Arg and Lys, in this region of Env (Fig. 2), as it has been shown that HLA-B*40:01

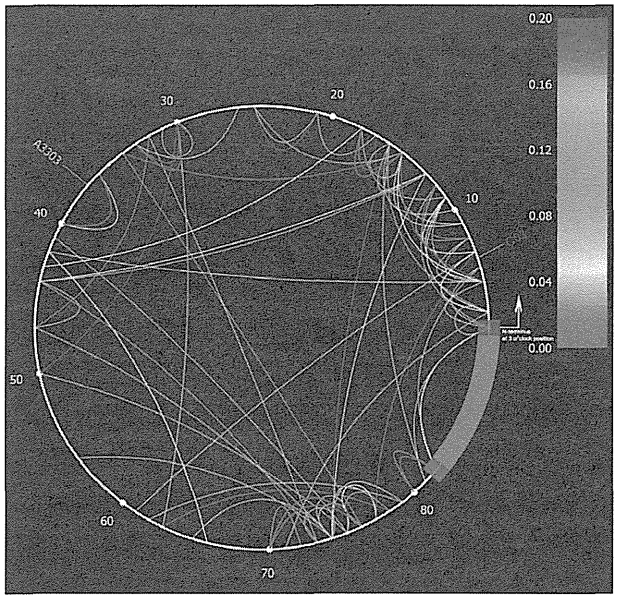

Fig. 3. Amino acid codon–codon covariation in Vpu. The circular map, generated by the PhyloDv software [13], shows Vpu codon–codon covariation associations as inner arcs connecting the association sites, with the HLA associations as tags pointing to their corresponding sites. Q values of individual codon pairs are represented as a heat map shown at the right.

preferentially binds peptides with acidic residues at their anchors [21]. This issue needs to be clarified in further studies using immunologic assays. Taken together, our results suggest that HLA-I-mediated selective pressure do not contribute to a large extent to population-level sequence variation in HIV-1 Vpu.

3.4. Codon–codon covariation of Vpu

Given that Vpu is functionally important in viral replication *in vivo*, the highly variable nature of Vpu amino acid sequences could be explained by complex networks of codon–codon covariation and/or secondary/compensatory mutation pathways. We therefore examined the codon–codon covariation of Vpu by using the phylogenetic dependency network model. Although Vpu consists of only 81 amino acids, we identified 103 covarying codon pairs in Vpu, displayed in Fig. 3. The covariation network in Vpu showed an uneven distribution, with a large number of codon–codon covariation networks at the N-terminal membrane-spanning region, a region responsible for BST-2 interaction [22]. Interestingly, the 3 HIV-HLA associations (Table 1, Fig. 2) were not significantly linked to any other amino acid residues. These data suggest that the conformation and function of Vpu may be preserved through many possible combinations of primary and secondary polymorphisms and that the HLA-I-associated immune-mediated selective pressure may have only a minor effect on such Vpu polymorphisms.

3.5. Association between Vpu polymorphisms and clinical parameters

Finally, we explored associations between Vpu polymorphisms and clinical parameters of HIV-infected patients (i.e., CD4 counts and plasma viral load). We observed no significant associations between Vpu polymorphisms and CD4 counts. However we identified a statistically significant association between amino acid residues at position 5 and viral load (Fig. 4). The patients harboring Val at Vpu-5 had significantly higher viral loads compared to those with amino acid residues other than Val at this position. Thus, amino acid residues at position 5 of Vpu showed several interesting features, i.e., the highest variability of all Vpu amino acids (Fig. 1A), nonadapted association of Glu-5 with *HLA-Cw*03*, and association of Val-5 with the increased viral load. Considering that the amino acid residue at this position is located in close proximity to the membrane-spanning region and that this region is functionally important for BST-2 binding, it would be interesting to examine functional effects of amino acid polymorphisms at position 5, whether they are mediated by host immune responses or otherwise.

In summary, we report here comparably fewer HLA-associated mutations in Vpu in this cohort although host HLA class I allele-associated immune responses are major forces driving the evolution of HIV-1 accessory proteins, such as Nef. Taken together, we conclude that the influence of immune selection on evolution of Vpu

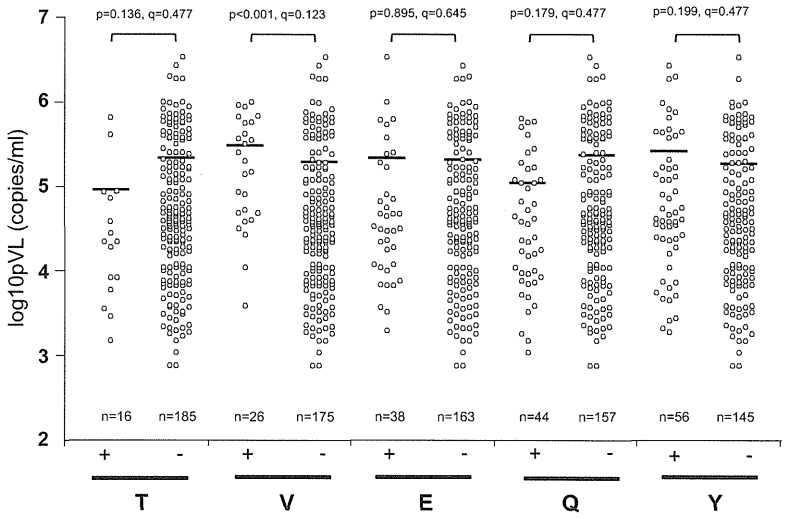

Fig. 4. Association between plasma viral load and amino acid polymorphism at position 5 of Vpu. HIV plasma viral loads, stratified by amino acid expression at Vpu codon 5, are shown. Vpu codon 5 exhibited 11 different amino acids positioning in our dataset; only those observed in >10 patients are shown here. Horizontal bars indicate medians. Statistical analysis was performed using the Mann-Whitney U-test.

at the population level may be reduced compared to other highly variable HIV-1 proteins, providing us with additional insight into differential evolutional pathways among viral accessory proteins.

Acknowledgments

This research was supported by a grant-in-aid for scientific research from the Ministry of Education, Science, Sports, and Culture (MEXT) of Japan, by a Global COE Program (Global Education and Research Center Aiming at the control of AIDS), MEXT, Japan, and by a grant-in-aid for AIDS research from the Ministry of Health, Labor, and Welfare of Japan. Z.H. is supported by the scholarship for The International Priority Graduate Programs; Advanced Graduate Courses for International Students (Doctoral Course), MEXT, Japan. Z.L.B. is the recipient of a New Investigator Award from the Canadian Institutes of Health Research.

References

[1] P.J.R. Goulder, D.I. Watkins, HIV and SIV CTL escape: implications for vaccine design, Nat. Rev. Immunol. 4 (2004) 630–640.
[2] C. Motozono, P. Mwimanzi, T. Ueno, Dynamic interplay between viral adaptation and immune recognition during HIV-1 infection, Protein Cell 1 (2010) 514–519.
[3] T. Bhattacharya, M. Daniels, D. Heckerman, B. Foley, N. Frahm, C. Kadie, J. Carlson, K. Yusim, B. McMahon, B. Gaschen, S. Mallal, J.I. Mullins, D.C. Nickle, J. Herbeck, C. Rousseau, G.H. Learn, T. Miura, C. Brander, B. Walker, B. Korber, Founder effects in the assessment of HIV polymorphisms and HLA allele associations, Science 315 (2007) 1583–1586.
[4] Z.L. Brumme, C.J. Brumme, D. Heckerman, B.T. Korber, M. Daniels, J. Carlson, C. Kadie, T. Bhattacharya, C. Chui, J. Szinger, T. Mo, R.S. Hogg, J.S. Montaner, N. Frahm, C. Brander, B.D. Walker, P.R. Harrigan, Evidence of differential HLA class I-mediated viral evolution in functional and accessory/regulatory genes of HIV-1, PLoS Pathog. 3 (2007) e94.
[5] Z.L. Brumme, M. John, J.M. Carlson, C.J. Brumme, D. Chan, M.A. Brockman, L.C. Swenson, I. Tao, S. Szeto, P. Rosato, J. Sela, C.M. Kadie, N. Frahm, C. Brander, D.W. Haas, S.A. Riddler, R. Haubrich, B.D. Walker, P.R. Harrigan, D. Heckerman, S. Mallal, HLA-associated immune escape pathways in HIV-1 subtype B Gag Pol and Nef proteins, PLoS One 4 (2009) e6687.
[6] C.B. Moore, M. John, I.R. James, F.T. Christiansen, C.S. Witt, S.A. Mallal, Evidence of HIV-1 adaptation to HLA-restricted immune responses at a population level, Science 296 (2002) 1439–1443.
[7] C.-A.M. Almeida, S.G. Roberts, R. Laird, E. McKinnon, I. Ahmad, N.M. Keane, A. Chopra, C. Kadie, D. Heckerman, S. Mallal, M. John, Exploiting knowledge of immune selection in HIV-1 to detect HIV-specific CD8 T-cell responses, Vaccine 28 (2010) 6052–6057.
[8] M. Dube, M.G. Bego, C. Paquay, E.A. Cohen, Modulation of HIV-1-host interaction: role of the Vpu accessory protein, Retrovirology 7 (2010) 114.
[9] M. Nomaguchi, M. Fujita, A. Adachi, Role of HIV-1 Vpu protein for virus spread and pathogenesis, Microbes Infect. 10 (2008) 960–967.
[10] K. Yusim, C. Kesmir, B. Gaschen, M.M. Addo, M. Altfeld, S. Brunak, A. Chigaev, V. Detours, B.T. Korber, Clustering patterns of cytotoxic T-lymphocyte epitopes in human immunodeficiency virus type 1 (HIV-1) proteins reveal imprints of immune evasion on HIV-1 global variation, J. Virol. 76 (2002) 8757–8768.
[11] M.M. Addo, M. Altfeld, A. Rathod, M. Yu, X.G. Yu, P.J. Goulder, E.S. Rosenberg, B.D. Walker, HIV-1 Vpu represents a minor target for cytotoxic T lymphocytes in HIV-1-infection, AIDS 16 (2002) 1071–1073.
[12] M. Altfeld, M.M. Addo, R. Shankarappa, P.K. Lee, T.M. Allen, X.G. Yu, A. Rathod, J. Harlow, K. O'Sullivan, M.N. Johnston, P.J.R. Goulder, J.I. Mullins, E.S. Rosenberg, C. Brander, B. Korber, B.D. Walker, Enhanced detection of human immunodeficiency virus type 1-specific T-cell responses to highly variable regions by using peptides based on autologous virus sequences, J. Virol. 77 (2003) 7330–7340.
[13] J.M. Carlson, Z.L. Brumme, C.M. Rousseau, C.J. Brumme, P. Matthews, C. Kadie, J.I. Mullins, B.D. Walker, P.R. Harrigan, P.J. Goulder, D. Heckerman, Phylogenetic dependency networks: inferring patterns of CTL escape and codon covariation in HIV-1 Gag, PLoS Comput. Biol. 4 (2008) e1000225.
[14] Y. Itoh, N. Mizuki, T. Shimada, F. Azuma, M. Itakura, K. Kashiwase, E. Kikkawa, J.K. Kulski, M. Satake, H. Inoko, High-throughput DNA typing of HLA-A, -B, -C, and -DRB1 loci by a PCR-SSOP-Luminex method in the Japanese population, Immunogenetics 57 (2005) 717–729.
[15] T. Ueno, Y. Idegami, C. Motozono, S. Oka, M. Takiguchi, Altering effects of antigenic variations in HIV-1 on antiviral effectiveness of HIV-specific CTLs, J. Immunol. 178 (2007) 5513–5523.
[16] T. Ueno, C. Motozono, S. Dohki, P. Mwimanzi, S. Rauch, O.T. Fackler, S. Oka, M. Takiguchi, CTL-mediated selective pressure influences dynamic evolution and pathogenic functions of HIV-1 Nef, J. Immunol. 180 (2008) 1107–1116.
[17] A. Bansal, J. Carlson, J. Yan, O.T. Akinsiku, M. Schaefer, S. Sabbaj, A. Bet, D.N. Levy, S. Heath, J. Tang, R.A. Kaslow, B.D. Walker, T. Ndung'u, P.J. Goulder, D. Heckerman, E. Hunter, P.A. Goepfert, CD8 T cell response and evolutionary pressure to HIV-1 cryptic epitopes derived from antisense transcription, J. Exp. Med. 207 (2010) 51–59.
[18] C.T. Berger, J.M. Carlson, C.J. Brumme, K.L. Hartman, Z.L. Brumme, L.M. Henry, P.C. Rosato, A. Piechocka-Trocha, M.A. Brockman, P.R. Harrigan, D. Heckerman, D.E. Kaufmann, C. Brander, Viral adaptation to immune selection pressure by HLA class I-restricted CTL responses targeting epitopes in HIV frameshift sequences, J. Exp. Med. 207 (2010) 61–75.
[19] D. Heckerman, C. Kadie, J. Listgarten, Leveraging information across HLA alleles/supertypes improves epitope prediction, J. Comput. Biol. 14 (2007) 736–746.
[20] K.C. Parker, M.A. Bednarek, J.E. Coligan, Scheme for ranking potential HLA-A2 binding peptides based on independent binding of individual peptide side-chains, J. Immunol. 152 (1994) 163–175.
[21] K. Falk, O. Rotzschke, M. Takiguchi, V. Gnau, S. Stevanovic, G. Jung, H.G. Rammensee, Peptide motifs of HLA-B58, B60, B61, and B62 molecules, Immunogenetics 41 (1995) 165–168.
[22] R. Vigan, S.J. Neil, Determinants of tetherin antagonism in the transmembrane domain of the human immunodeficiency virus type 1 Vpu protein, J. Virol. 84 (2010) 12958–12970.

Viruses **2012**, *4*, 1711-1730; doi:10.3390/v4091711

OPEN ACCESS

viruses

ISSN 1999-4915

www.mdpi.com/journal/viruses

Review

Human Leukocyte Antigen (HLA) Class I Down-Regulation by Human Immunodeficiency Virus Type 1 Negative Factor (HIV-1 Nef): What Might We Learn From Natural Sequence Variants?

Philip Mwimanzi [1], Tristan J. Markle [1], Takamasa Ueno [2] and Mark A. Brockman [1,3,*]

[1] Department of Molecular Biology and Biochemistry, Simon Fraser University, 8888 University Drive, Burnaby, British Columbia V5A 1S6, Canada; E-Mails: pwimanzi@sfu.ca (P.M.); tmarkle@sfu.ca (T.J.M.)

[2] Center for AIDS Research, Kumamoto University, 2-2-1 Honjo, Chuo-ku, Kumamoto 860-0811, Japan; E-Mail: uenotaka@kumamoto-u.ac.jp

[3] Faculty of Health Sciences, Simon Fraser University, 8888 University Drive, Burnaby, British Columbia V5A 1S6, Canada

* Author to whom correspondence should be addressed; E-Mail: mark_brockman@sfu.ca; Tel.: +1-778-782-3341; Fax: +1-778-782-5583.

Received: 31 August 2012; in revised form: 18 September 2012 / Accepted: 21 September 2012 / Published: 24 September 2012

Abstract: HIV-1 causes a chronic infection in humans that is characterized by high plasma viremia, progressive loss of CD4+ T lymphocytes, and severe immunodeficiency resulting in opportunistic disease and AIDS. Viral persistence is mediated in part by the ability of the Nef protein to down-regulate HLA molecules on the infected cell surface, thereby allowing HIV-1 to evade recognition by antiviral CD8+ T lymphocytes. Extensive research has been conducted on Nef to determine protein domains that are required for its immune evasion activities and to identify critical cellular co-factors, and our mechanistic understanding of this process is becoming more complete. This review highlights our current knowledge of Nef-mediated HLA class I down-regulation and places this work in the context of naturally occurring sequence variation in this protein. We argue that efforts to fully understand the critical role of Nef for HIV-1 pathogenesis will require greater analysis of patient-derived sequences to elucidate subtle differences in immune evasion activity that may alter clinical outcome.

Keywords: HIV-1; Nef; immune evasion; HLA class I; cytotoxic T lymphocyte; viral sequence diversity; host immune selection pressure

1. Introduction

This review discusses our current knowledge of the Human immunodeficiency virus type 1 (HIV-1) Negative Factor (Nef) protein and its ability to mediate immune evasion through down-regulation of Human Leukocyte Antigen class I (HLA-I) molecules on the surface of virus-infected cells. We highlight recent evidence based on cellular, molecular, and structural biology studies that extends our mechanistic understanding of this important Nef activity. Furthermore, the relevance of naturally occurring Nef sequence variation and it potential impact on protein function and clinical outcome is presented. We emphasize the critical need to examine Nef function using patient-derived viral sequences in order to fully understand the role that Nef plays in HIV-1 pathogenesis.

1.1. HIV-1 Infection and Therapy

HIV-1 causes a life-long infection that is characterized by the rapid destruction of gut lymphoid compartments [1–3] followed by the progressive loss of peripheral blood CD4+ T lymphocytes [4]. The ultimate outcome of infection is a severe decline of the host immune system that is observed clinically as the inability to control opportunistic pathogen infections–a condition that is commonly referred to as acquired immunodeficiency syndrome (AIDS) [4]. Over the past 30 years, a large number of antiviral drugs have been developed that target essential stages in the HIV-1 replication cycle, including enzymatic processes (e.g., reverse transcriptase, protease, and integrase inhibitors) and critical viral:host protein interactions (e.g., CCR5 co-receptor antagonists) [5]. Advances in highly active antiretroviral therapy (HAART) have significantly reduced the burden of HIV/AIDS in regions of the world where these potent drug combinations are available, and HAART is currently our best option to control the spread of HIV [6,7]; however, establishment of latent viral reservoirs and ongoing low-level viremia in treated individuals require that therapy be continued for life. An improved understanding of the mechanisms that allow HIV-1 to persist and cause disease in its human host may uncover new opportunities for clinical or therapeutic intervention [8].

1.2. The Nef Protein

The HIV-1 accessory protein Nef is necessary for viral pathogenesis and progression to AIDS. Its *in vivo* role was first illustrated in the rhesus macaque model system where a *nef*-deleted strain of simian immunodeficiency virus (SIV) exhibited reduced viral replication, lower plasma viremia, and attenuated pathogenicity [9]. *Nef* gene deletion has also been associated with non-progressive HIV-1 infection [10,11]. Several reports have attempted to correlate Nef sequence polymorphisms with clinical outcome [12,13], with mixed results; however, relatively few studies have assessed potential functional impairment of Nef in the context of progressive or non-progressive HIV-1 infection using patient-derived sequences [14–17], and each of these reports examined only a small number of individuals.

HIV-1 Nef is a ~27kd protein that is expressed abundantly during the early stages of viral replication [18]. Nef displays diverse *in vitro* functions, including the ability to modulate a number of cell surface proteins [19], augment viral infectivity, and enhance viral replication capacity [20,21]. Down-regulation of host cell CD4 [22,23] and HLA-I [24,25] surface molecules are the most extensively studied of Nef's activities, although some of its functions may share overlapping mechanisms. For example, Nef CD4 down-regulation activity correlates with its ability to enhance viral pathogenesis [26,27]; and lower CD4 expression on virus-infected cells may directly increase viral infectivity [28], virion release [29], viral replication [30], or prevent superinfection [31–33]. Although Nef's contributions to HIV-1 pathogenesis remain incompletely understood, it has been proposed that progressive disease may require a combination of Nef-mediated functions acting at different times during the infection course [34,35].

1.3. HIV-1 Immune Evasion Strategies

HIV-1 evades host cellular immune responses through Nef-dependent and Nef-independent mechanisms. Nef-mediated down-regulation of HLA-I protects virus-infected cells from recognition by CD8+ T lymphocytes [36], but modulation of other host cell proteins, including CD4, CD8ß, CD28, CD74 (invariant chain), and HLA class II, may also contribute to Nef-dependent immune evasion [19,37,38]. Nef-independent immune evasion relies on the generation of viral sequence polymorphisms ("escape mutations") within or near targeted epitopes, resulting in directional evolution of the virus away from immune selection pressure [39,40]. Despite these evasion strategies, CTL may retain antiviral activity, particularly if they recognized viral epitopes that can be presented prior to Nef-induced HLA-I down-regulation [41]. Nef selectively modulates HLA-A and HLA-B alleles through a shared sequence ($Y_{320}SQAASS_{326}$) located in their cytoplasmic tail [42,43], leaving HLA-C allele expression unchanged on the cell surface presumably to counter the innate Natural Killer cell response against HLA-devoid cells [44]. Recent data, however, suggests that Nef-mediated down-regulation of HLA-B is less robust than that of HLA-A [45], which may in part explain the observation that HLA-B alleles tend to be more protective against HIV-1 disease progression *in vivo* [46].

2. HLA Class I-Mediated Control of HIV-1

2.1. Role of HLA-I in Viral Infection

During the course of viral infection, the cellular proteasome complex degrades viral proteins to produce immunogenic peptide antigens. These cytosolic peptides are transported into the endoplasmic reticulum (ER), captured by HLA-I proteins, and traffic to the cell surface for presentation to circulating antiviral CD8+ cytotoxic T lymphocytes (CTL) (Figure 1). Antigen-specific T cell receptors (TCR) allow a subset of CTL to recognize these "non-self" peptides bound to HLA on the infected cell surface. Following TCR engagement with its HLA/peptide ligand, the CTL forms an "immunological synapse" with the target cell and releases antiviral cytokines and cytotoxic molecules, including perforin and granzymes, to eliminate the infected cell [47].

Figure 1. Presentation of viral peptide antigens by Human Leukocyte Antigen (HLA) class I. Human immunodeficiency virus type 1 (HIV-1) proviral gene expression, including RNA transcription (**a**) and protein translation (**b**); generates functional viral proteins (**c**) as well as truncated or mis-folded proteins that are degraded by the cellular proteasome complex to form short antigenic peptides (**d**); These peptides are transported from the cytoplasm into the endoplasmic reticulum (ER) (**e**) where they can be loaded onto HLA-I molecules. Peptide/HLA complexes traffic from the ER through the Golgi and secretory vesicle (SV) network to the plasma cell membrane, where the peptide antigens are presented to circulating cytotoxic T lymphocytes (CTL) (**f**); The viral Nef protein shuttles HLA molecules located at the cell surface or within the *trans*-Golgi network into lysosomal compartments (**g**); where they are degraded. In the absence of Nef-mediated HLA down-regulation, antigen-specific CTL respond to stimulation by releasing cytotoxic molecules, including perforin and granzymes, resulting in elimination of the virus-infected cell (h).

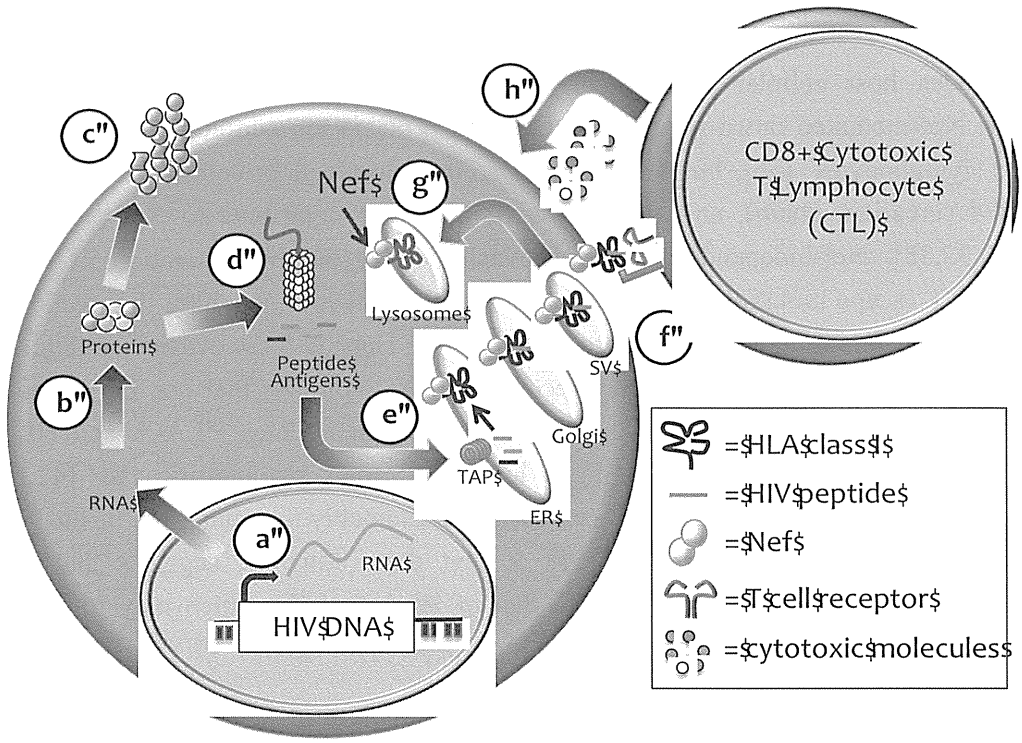

The critical role of HLA-I in control of infection is illustrated by the variety of strategies that viruses have independently developed in order to evade HLA-dependent immune responses [40,48–50]. In the case of HIV-1, Nef down-regulates HLA-A and B alleles on the cell surface and thereby reduces viral peptide presentation to CTL [19,49]. HIV-1 sequences also undergo mutational escape in an HLA-restricted manner, yielding epitope variants that are incompletely or improperly processed, presented and/or recognized by CTL [39,40].

2.2. HLA Class I as a Major Determinant of HIV-1 Pathogenesis

Rates of clinical disease progression during natural HIV-1 infection vary widely, and this has been attributed mainly to differences in HLA-restricted CTL responses [40,51,52]. The association of CTL responses with initial control of plasma viremia during primary HIV-1 infection [53,54], delayed

disease progression [55] and the observation that rhesus macaques depleted of CD8+ cells prior to SIV infection exhibited an inability to control viremia [56] strongly support a critical role for CTL in control of HIV-1 at early times following infection. Over the course of infection, CTL selection pressure results in the generation of viral escape variants [53], and HLA-restricted CTL responses are a major selective force driving viral evolution in an infected host [39]. As a result of immune escape and immune dysfunction, CTL ultimately fail to control infection and the vast majority of individuals' progress to AIDS in the absence of HAART.

HIV-1 long-term non-progressors (LTNP) and spontaneous controllers have been carefully examined in order to elucidate mechanisms of viral pathogenesis and to identify novel correlates of immune-mediated protection. It has been observed that "protective" HLA-I alleles, most notably B*27 and B*57, are consistently associated with enhanced control of HIV [57]. More recently, genome-wide association studies (GWAS) have identified single-nucleotide polymorphisms (SNPs) in the HLA region on human chromosome 6 as major determinants of lower plasma viral load set point [58,59] as well as the HIV elite controller phenotype [60–62]. Understanding potential differences in the ability of Nef to modulate CTL responses in the context of different HLA alleles or viral peptides is an area of research that merits further attention [45,63].

3. Nef-Dependent Immune Evasion: *In Vivo* and *in Vitro* Observations

In vivo observations have clearly suggested that Nef plays a critical role for maintenance of high plasma viremia and for progression to AIDS [9–11]; however, evidence to directly link Nef-mediated HLA-I down-regulation to clinical outcome is more limited. Studies using the SIV-infected macaque model system have observed that Nef mutations that impaired HLA down-regulation activity were restored during the course of infection [64,65], and it was recently shown that high plasma viremia following SIV infection correlated with a high level of *in vivo* HLA-I down-regulation [66]. Similarly, it has been reported that patient-derived Nef sequences collected during early or chronic HIV-1 infection retained significant ability to down-regulate HLA-I and to evade CTL killing [16,67]; however, other data indicate that this function may be dispensable during very late stage disease [34]. Altogether, these results indicate that HLA down-regulation is a very important *in vivo* Nef function that is maintained presumably in order to evade ongoing CTL immune pressure on the virus.

In vitro studies from a number of research groups have observed substantial variation in the susceptibility of HIV-infected cells to recognition and killing by CTL using standard co-culture assays [36,68–70]. This result is likely due to the use of different target cells, different CTL clones, and viral strains that may encode Nef variants with differential levels of expression or subtle differences in HLA down-regulation function. In cases where CTL-mediated recognition or killing has been compared directly between HIV strains that encode the *nef* gene *versus* variants harboring deletions or non-functional alleles, Nef expression has clearly been shown to confer a protective effect in both cell lines and in primary T cell assays [36,63,70–72]. Notably, even though Nef effectively reduces CTL-mediated killing of virus-infected cells, it may not fully abrogate the ability of responding CTL to produce antiviral chemokines or cytokines [63]. While such incomplete evasion of CTL permits non-cytolytic immune mechanisms to participate in control of chronic infection [73], it

nevertheless allows HIV-1 to establish a persistent infection in the face of robust antiviral host immunity.

4. Nef Structure and HLA Class I Down-Regulation Function

4.1. General Features of Nef and its Domain Structure

Nef serves as an adaptor protein and its various functions appear to utilize non-canonical motifs and interactions to form higher-order complexes with cellular proteins [74]. Despite its small size, Nef engages with multiple and diverse host cell proteins, thereby altering their normal function to favor viral replication. Biochemical characterization of these protein complexes remains difficult, likely due to the small size of Nef, the heterogeneous nature of the complexes that are formed, and the localization of these complexes within lipid membranes.

The protein structure of Nef can be broadly divided into three domains: an N-terminal anchor and flexible loop, a central structured core, and a C-terminal flexible loop [75,76]; and two amino acid positions have been shown to be particularly critical for Nef function. The N-terminal anchor domain of Nef is required for membrane association and localization into detergent-insoluble "lipid rafts" [77], while the central core encodes numerous protein interaction and intracellular trafficking motifs that contribute differentially to diverse Nef functions [78]. The central core domain of Nef adopts a stable tertiary fold, permitting its early characterization using both NMR and X-ray crystallographic
methods [79,80]. Our understanding of Nef-mediated HLA down-regulation has been significantly enhanced by the recently reported crystal structure of Nef protein in complex with the MHC-I cytoplasmic domain and the μ1 subunit of the clatherin AP1 complex [76].

4.2. Functional Motifs and Host Proteins Interactions

Myristoylation at glycine residue 2 (G_2) allows the Nef protein to localize to lipid membranes, including the inner leaflet of the plasma membranes [81] and aspartic acid residue 123 (D_{123}) is reported to be necessary for protein oligomerization [82]. Recent data also suggest that electrostatic interactions at D_{123} may be essential for Nef stability [76]. Site-directed mutations at either residue G_2 or D_{123} have been shown to impair nearly all known Nef activities [82,83], however most other mutations indicate that the functional motifs required to down-regulate HLA-I are genetically separable from those required to modulate CD4. Notably, sequences in the central core domain that bind to the clatherin adaptor protein complex AP-2 [84,85], the coatomer protein ß-COP [86,87], and the vacuolar membrane ATPase V1H [88,89] are necessary for down-regulation and degradation of CD4 [90], but not HLA-I.

The ability of Nef to down-regulate HLA-I surface expression [24,91,92] has been mapped to three distinct regions of the protein. First, an N-terminal alpha helix ($R_{17}ER_{19}M_{20}RRAEPA_{26}$) that contains methionine residue 20 (M_{20}) serves an important as a membrane anchor [90,93], and more recently arginine residues 17 and 19 have been shown to form a second ß-COP binding motif [87]. This latter observation indicates that the final stages of Nef-mediated CD4 and HLA down-regulation may need to engage the same cellular machinery and lysosomal compartments. Second, an acidic cluster

($E_{62}EEE_{65}$) that binds to the PACS-1 and PACS-2 proteins may enhance Nef localization to the *trans*-Golgi network (TGN) and/or regulate signaling events that increase the rate of cellular endocytosis [94,95]. Finally, a polyproline $(PxxP)_3$ repeat that includes proline residues 72, 75, and 78 forms an SH3-binding motif that has been shown to interact with Lyn and Hck cellular kinases [90].

4.3. Proposed Mechanisms of HLA Class I Down-Regulation

Two models to explain Nef-mediated HLA-I down-regulation are currently favored, including (1) altered HLA trafficking and (2) enhanced HLA internalization/turnover. These proposed mechanisms are not mutually exclusive, and indeed the two may function collaboratively within the virus-infected cell to ensure robust immune evasion.

In the 'altered trafficking' model, interaction between Nef and newly synthesized HLA-I occurs within the secretory pathway, disrupting normal HLA-I transport to the cell surface and redirecting it to endosome/lysosome compartments for degradation. There is strong evidence to support this model, such as the observation that Nef and HLA-I co-localize within the trans-Golgi network rather than at the cell membrane [95]. In addition, direct binding has been demonstrated between Nef and a number of cellular complexes, including AP-1 [96] and ß-COP [86]. These complexes are necessary for normal protein transport between the trans-Golgi and endosomes, and mutations in Nef that disrupt these domains dramatically impair HLA-I down-regulation function. Further support comes from biochemical data indicating that the μ1 subunit of AP-1 forms a stable interaction with Nef only in the presence of the HLA-I cytoplasmic tail [97–99]. The interaction between Nef and the AP-1 complex is thought to allow the μ subunit of AP-1 (which typically recognizes YxxØ motifs; where Ø is a bulky hydrophobic residue and x is any amino acid) to associate with a non-conventional sequence ($Y_{320}SQA_{323}$) in the cytoplasmic tail of HLA-I [42,99,100]. This hypothesis has been validated recently by structural determination of the Nef/μ1/HLA tripartite complex at less than 3-angstrom resolution [76], which captured this complicated interaction 'in action'. Notably, this new structure demonstrates that a highly cooperative interaction between Nef and μ1 creates a novel binding pocket on μ1 that can accommodate a YxxA motif in HLA-I cytoplasmic tail. More specifically, Nef's acidic cluster, $E_{62}EEE_{65}$, provides critical electrostatic interactions with μ1 that stabilize the complex and Nef's polyproline-rich motif, PxxP, acts as a clamp to secure binding of HLA-I to μ1. These results confirm previous models based largely on biochemical data and provide clear rationale for the role of these Nef sequences in its HLA-I down-regulation activity. Furthermore, the structure by Jia *et al.* [76] highlights an important role for hydrophobic residues located in Nef's N-terminal and C-terminal domains. While not participating directly in HLA-I or μ1 binding, Nef residues W_{13} and M_{20} anchor the protein core to the plasma membrane and presumably help to position Nef appropriately for optimal interactions with its binding partners. Likewise, residues Y_{202} and F_{203} appear to stabilize the HLA-I tail interaction.

In the 'enhanced turnover' model, Nef is thought to act through a series of interactions and signaling events to induce clatherin-independent internalization of HLA-I at the plasma cell membrane that requires small GTPases known as ADP-ribosylation factors (ARFs). It is proposed that Nef's $E_{62}EEE_{65}$ motif binds to the phosphofurin acidic cluster sorting protein PACS-2 and localizes Nef within the *trans*-Golgi network (TGN) [94,95]. This allows Nef to bind to Src-family protein kinases

in the TGN (in particular Hck) [101], triggering a signaling pathway that includes activation of the tyrosine kinase protein ZAP70 and PI-3-kinase, induction of phosphotidylinositol-3-phosphate (PIP_3) on the inner leaflet of the plasma membrane, and PIP_3-mediated recruitment of ARNO [102], that culminates in activation of ARF-6 that results in endocytosis of HLA-I [103]. Several aspects of this model remain controversial, and more recent studies have shown only modest effect of specific ARF-6 inhibitors [104] or a dominant-negative ARF6 mutant [105] on Nef-mediated HLA-I down-regulation.

The unusual functional flexibility of Nef is demonstrated by the fact that both of these HLA-I down-regulation models differ significantly from the mechanism that Nef uses to modulate CD4 expression, reviewed in [74,106]. In that case, direct interactions between Nef, the cytoplasmic tail of CD4, and the AP-2 complex at the plasma membrane [107] results in clatherin-mediated endocytosis of CD4 and its eventual degradation in lysosomes.

5. Natural Variation in Nef Sequence and Implications for Immune Evasion

5.1. Sequence Variability within Described HLA-I Down-Regulation Motifs

Nef is one of the most highly variable HIV-1 proteins; however, the impact of naturally occurring mutations on clinical outcome has rarely been explored in detail [12,108]. This is due, in part, to the fact that many of the motifs associated with its HLA-I down-regulation function are very well conserved in patient-derived sequences [12,109]. Analysis of a panel of 242 HIV-1 subtype B Nef sequence clones obtained from unique individuals by our laboratory (68 from acute infection, 122 in chronic infection, and 52 spontaneous controllers with plasma viral load <50 copies RNA/mL; *unpublished data*) confirms these previous observations (Table 1). The frequency of the consensus amino acid as well as the Shannon entropy value for each critical residue was determined using web-based tools available at the Los Alamos National Laboratory HIV Sequence Database [110]. Notably, we observed that the Nef residues required for HLA-I down-regulation function–including myristoylation (G_2 and S_6) and putative stability (W_{13}), proline residues P_{72}, P_{75}, and P_{78} in the $(PxxP)_3$ domain, and the aspartic acid residue D_{123}–were essentially unchanged in all patient-derived sequences (all frequencies >99%). While other critical Nef residues displayed less conservation, only glutamic acid residues E_{63} and E_{64} were observed to occur in less than 90% of sequences in this cohort of individuals with broad clinical outcome. These changes were mainly conservative substitutions to aspartic acid that are expected to have modest effect on Nef function based on previous studies [111], indicating that population-level variation in the acidic domain may also be limited.

Nef sequences adjacent to known motifs tend to be more variable, but their role in Nef function remains largely unexplored. In addition to P_{72}, P_{75}, and P_{78}, mutations at residues Q_{73}, V_{74}, L_{76}, and R_{77} in the $(PxxP)_3$ motif have been shown to alter Nef function [112–114]; however, each of these residues is highly conserved in our patient-derived sequences (Table 1). Greater diversity is observed in the N-terminal motif of Nef, with consensus residues R_8, S_9, V_{10}, and V_{11} displaying less than 70% identity in our cohort (all entropy scores >1.0; *data not shown*). Similarly, we observed substantial variability in the C-terminal loop, where Y_{202} and Y_{203} displayed frequencies of ~90%. Finally, a number of Nef codons were shown recently by Lewis *et al.* [115] to be subject to strong purifying

selection pressure by CTL and to impair Nef's HLA down-regulation function, including novel polymorphisms N52A, A84D, Y135F, G140R, S169I, and V180E that displayed a range of diversity in our patient sequences. More detailed studies of these regions are warranted to fully explore the possibility that common changes in Nef sequence may affect clinical outcome.

Table 1. Sequence conservation in HIV-1 negative factor (Nef) motifs required for HLA-I down-regulation.

Nef Domain [a]	Role	AA	Frequency [b]	Entropy [b]	References
MG_2xxxS_6	Myristoylation	G_2	100 %	0	[116]
		S_6	99.2 %	0.05	[116]
W_{13}	Stability (?)	W_{13}	100 %	0	[76]
$R_{17}xR_{19}$	ß-COP	R_{17}	97.5 %	0.15	[87]
		E_{18}	96.7%	0.18	[115]
		R_{19}	90.5 %	0.35	[87]
M_{20}	Stability (?)	M_{20}	90.5 %	0.37	[93]
?	Unknown	N_{52}	98.8%	0.08	[115]
$E_{62}EEE_{65}$	PACS-1/2	E_{62}	92.1 %	0.31	[95,115]
		E_{63}	75.2 %	0.72	[95]
		E_{64}	88.8 %	0.48	[95]
		E_{65}	91.7 %	0.35	[95]
$P_{72}xxPxR_{77}$	SH3 binding,	P_{72}	100 %	0	[76,81,117]
and $(PxxP)_3$	HLA-I "clamp"	Q_{73}	99.6 %	0.03	[76,81,117]
		V_{74}	99.4 %	0.05	[76,81,115,117]
		P_{75}	100 %	0	[76,81,117]
		L_{76}	96.7 %	0.16	[76,81,117]
		R_{77}	100 %	0	[76,81,117]
		P_{78}	99.6 %	0.03	[76,81,117]
		G_{83}	56.2%	0.73	[90,115]
?	Unknown	A_{84}	99.2%	0.05	[115]
D_{123}	Oligomerization and Stability (?)	D_{123}	100 %	0	[74,76,82,115]
?	Unknown	Y_{135}	75.2%	0.64	[115]
?	Unknown	G_{140}	100%	0	[76,115]
?	Unknown	S_{169}	89.7%	0.47	[76,115]
D_{175}	Trafficking	D_{175}	99.6%	0.03	[76,88,115,118]
?	Unknown	V_{180}	99.2%	0.05	[76,115]
Y_{202}	Stability (?)	Y_{202}	87.6 %	0.39	[76]
F_{203} [c]	Stability (?)	F_{203}	9.5 %	0.31	[76]
		Y_{203}	90.5 %	0.31	[76]
D_{123}	Oligomerization and Stability (?)	D_{123}	100 %	0	[74,76,82,115]
?	Unknown	Y_{135}	75.2%	0.64	[115]
?	Unknown	G_{140}	100%	0	[76,115]
?	Unknown	S_{169}	89.7%	0.47	[76,115]
D_{175}	Trafficking	D_{175}	99.6%	0.03	[76,88,115,118]

[a]: Protein locations based on HXB2 numbering [110]; [b]: Frequency of consensus residue and Shannon entropy score calculated using 242 clonal Nef sequences collected from unique HIV-1 subtype B-infected individuals from North America (68 acute, 122 chronic, and 52 controllers) and the Entropy-One tool (HIV Sequence Database; [110]);
[c]: Nef used by Jia *et al.* [76] encoded phenylalanine-203, but tyrosine-203 is prevalent in most sequences.